Stability of fronts for a regularization of the Burgers equation

H. S. Bhat* R. C. Fetecau†

January 25, 2007

Abstract

We consider the stability of traveling waves for the Leray-type regularization of the Burgers equation that was recently introduced and analyzed by the authors in [BF]. These traveling waves consist of "fronts", which are monotonic profiles that connect a left state to a right state. The front stability results show that the regularized equation mirrors the physics of rarefaction and shock waves in the Burgers equation. Regarded from this perspective, this work provides additional evidence for the validity of the Leray-type regularization technique applied to the Burgers equation.

1 Introduction

The following regularization for the Burgers equation was introduced and analyzed by the authors in [BF]:

$$v_t + uv_x = 0, \tag{1a}$$

$$v = u - \alpha^2 u_{xx}, \tag{1b}$$

where $\alpha > 0$ is a constant that has dimension of length. Subscripts denote differentiation. By introducing the Helmholtz operator

$$\mathcal{H} = \mathrm{Id} - \alpha^2 \partial_x^2, \tag{2}$$

we may rewrite (1a) as

$$v_t + \left[\mathcal{H}^{-1} v\right] v_x = 0.$$

If one thinks of the inviscid Burgers equation $v_t + vv_x = 0$ as a transport equation with local transport velocity equal to v itself, then the regularization (1) consists of using a smoothed or filtered version of v—specifically $\mathcal{H}^{-1}v$—in place of v. This regularization idea was first employed by Leray in 1934 [Ler34]. Working in the context of the incompressible Navier-Stokes equations, Leray proposed replacing the nonlinear term $(v \cdot \nabla)v$ with a term $(u \cdot \nabla)v$. Here $u = K^\epsilon * v$ for some smoothing kernel K^ϵ. Leray's program consisted in proving existence of solutions for his modified equations and then showing that these solutions converge, as $\epsilon \downarrow 0$, to weak solutions

*Applied Physics and Applied Mathematics, Columbia University, New York, NY 10027 (hsb2106@columbia.edu)

†Department of Mathematics, Simon Fraser University, Burnaby, BC V5A 1S6, Canada (van@math.sfu.ca)

of Navier-Stokes—see [Ler34] for details. The idea of using a Leray-type regularization in lieu of dissipation, for the purposes of capturing shocks in the Burgers equation, was suggested independently by J. E. Marsden, K. Mohseni [MZM06], and E. S. Titi.

As we demonstrated in [BF], system (1) is globally well-posed with initial data $v(x,0)$ in the Sobolev space[1] $W^{2,1}(\mathbb{R})$. Using a combination of analysis and numerics, we showed that solutions $u^\alpha(x,t)$ of (1) converge strongly, as $\alpha \to 0$, to entropy solutions of the inviscid Burgers equation. In the present paper we prove stability (in some sense) for *monotone decreasing* fronts and instability for *monotone increasing* fronts. These two types of traveling fronts correspond, respectively, to viscous shocks and rarefaction waves. Our results match existing results regarding the stability of viscous shock profiles in hyperbolic conservation laws [Sat76, Goo86]. However, the existing literature on the stability of traveling waves does not deal with system (1). Our purpose here is to remedy this gap, and thereby strengthen the connection between the Leray-type regularization (1) and standard viscous regularizations of $v_t + vv_x = 0$.

System (1) also appears in the works of Holm and Staley [HS03a, HS03b] as a model for one-dimensional nonlinear wave dynamics in fluids. More precisely, system (1) is the $b = 0$ member of the b-family of fluid transport equations,

$$v_t + uv_x + bu_x v = 0, \tag{3a}$$

$$u = G * v. \tag{3b}$$

In (3), $u(x,t)$ stands for velocity, $v(x,t)$ for momentum density, and $G(x)$ for an even kernel function that relates v and u by convolution.

Specifically, the b-family (3) includes the effects of convection, represented by the term uv_x, and stretching, represented by $u_x v$. The dimensionless parameter b measures the relative strength of these effects. When linear dispersion and viscosity terms are added, (3) appears in asymptotic studies of the shallow water equations, and we refer the reader to [DGH01, DGH03, DGH04] for further discussions in this direction. One common point of such physically motivated studies is that the kernel G takes the form

$$G(x) = \frac{1}{2}\exp(-|x|/\alpha), \tag{4}$$

which implies that u and v are related by (1a).

Let us remind the reader that the $b = 2$ case of (3) is the Camassa-Holm equation [CH93], while the $b = 3$ case is the Degasperis-Procesi equation [DP99]. At the time of writing, there have been hundreds of papers written on these equations, and we will not attempt a review of that literature here. It is sufficient to say that quite a lot of the interest behind these equations stems from their complete integrability, and, related to this, their peakon solutions. Peakons are the spatially localized, peaked, traveling wave solutions of (3) given by $u(x,t) = \exp(-|x - ct|/\alpha)$; interactions between N peakons are governed by a completely integrable finite-dimensional dynamical system. Stability of Camassa-Holm peakons and solitary waves was considered in [CS00, CS02].

Here we focus exclusively on non-peakon solutions of the $b = 0$ case of (3a), which take the form of *traveling fronts*: monotone waves $u(x,t) = f(x - ct)$ that connect a left state

[1] In fact, what we showed is slightly stronger than this. Initial data $v_0(x)$ that is continuously differentiable, with two weak derivatives $v_0', v_0'' \in L^1(\mathbb{R})$ yields global well-posedness.

$u(-\infty, t) = u_L$ to a right state $u(+\infty, t) = u_R$, with $u_L \neq u_R$. Such front solutions were derived and studied numerically in [HS03a, HS03b]; our contribution here is the first analytical treatment of their stability. We treat, in turn, questions of linear, spectral, and nonlinear stability. We also carry out a numerical study of the orbital stability of the fronts.

There are some intriguing difficulties for non-local nonlinear PDE such as (1). We say the PDE is non-local because it can be written in the convective form

$$u_t + uu_x = -\frac{3}{2}\alpha^2 \partial_x \mathcal{H}^{-1} u_x^2, \tag{5}$$

with the Helmholtz operator $\mathcal{H}$ defined by (2).

Though it is known that the b-family has a non-local Poisson structure [DHH03, HW03, HH05], we have shown [BF] that there are no Casimirs associated to the $b = 0$ version of this structure. Furthermore, though the quantities

$$\int_{\mathbb{R}} u(x,t)\,dx, \quad \int_{\mathbb{R}} v(x,t)\,dx, \quad \|v(\cdot,t)\|_{L^\infty}, \quad \|v_x(\cdot,t)\|_{L^1} \tag{6}$$

are constant on solutions of (1), none of these invariants help us frame the traveling fronts as critical points of an appropriate functional. We are unaware of invariants besides the ones mentioned in (6), and also unaware of the Lagrangian/variational counterpart to the non-local Poisson structure underlying (1).

The upshot is that certain standard methods for proving stability for nonlinear systems may not be applicable for system (1). Also, the front traveling waves (defined below in (8)) are only *weak* (distributional) solutions of (1) and this fact makes the stability study very non-standard and challenging.

Our analysis makes use of the following symmetries of (1):

- Dilation: for any $\alpha > 0$, the function $U(x,t)$ solves (1) if and only if

  $$u(x,t) = U(\alpha x, \alpha t)$$

  solves the system

  $$v_t + uv_x = 0, \tag{7a}$$
  $$v = u - u_{xx}. \tag{7b}$$

  In what follows we consider the "$\alpha = 1$" system (7) only.

- Galilean invariance: first let us step back and note that all traveling front solutions of (7) are given by

  $$u^0(x,t) = \begin{cases} u_L + d\exp(x - ct) & x < ct \\ u_R - d\exp(-(x - ct)) & x > ct, \end{cases}$$

  where c is the speed of the front and $u_L = c - d$, $u_R = c + d$ are the boundary values at $x = -\infty$ and $x = \infty$, respectively.

System (7) is Galilean invariant[2], i.e. invariant under the mapping $(x,u) \mapsto (x+u_0t, u+u_0)$. In precise terms, if $u(x,t)$ solves (7a), then so does $\overline{u}(\overline{x},t) = u(\overline{x}-u_0t,t)+u_0$, for any $u_0 \in \mathbb{R}$. Hence we can eliminate the wave speed c from the proceedings and consider the stationary solutions ($c=0$) only, i.e.

$$u^0(x) = d\bar{u}^0(x) = d\begin{cases} -1+\exp(x) & x<0, \\ 1-\exp(-x) & x>0. \end{cases} \tag{8}$$

Here $\bar{u}^0$ is the the "normalized" standing wave solution.

- Parity: as noted in [HS03b, §3.4], system (7) is invariant under the reflections $u(x,t) \mapsto -u(-x,t)$. Assuming existence and uniqueness of solutions, this implies that odd initial data $u(x,0)$ evolves into a solution $u(x,t)$ that remains odd for all $t>0$. We reserve further discussion on this symmetry for later when we actually utilize it.

We also make use of the non-local form (5) together with the method of characteristics, especially when looking into nonlinear stability of fronts.

Overview and Roadmap. In this paper, we prove the following results regarding the stationary front solutions (8) of (7).

- Linear stability of the $d<0$ (monotone decreasing) fronts
- Linear instability of the $d>0$ (monotone increasing) fronts
- Nonlinear asymptotic stability of the $d<0$ fronts with respect to perturbations f such that u^0+f is strictly decreasing and odd.

Additionally, we provide numerical evidence that:

- The $d<0$ fronts are orbitally stable.

The paper is organized as follows: in Section 2, we formulate precisely the stability problem under investigation. Stability/instability in the linearized problem is covered in Section 3, while nonlinear stability is discussed in 4. In Section 5, we study numerically the orbital stability of traveling fronts. The Appendix contains the detailed computation regarding the solution presented in Section 3.1.

2 Problem formulation

Regularity of traveling waves. Before looking into stability questions, we must mention that the traveling front solutions (8) are actually global-in-time *weak* solutions of (7). The weak form of (7a) follows naturally from the conservation law

$$v_t + \left(\frac{1}{2}u^2 - uu_{xx} + \frac{1}{2}u_x^2\right)_x = 0. \tag{9}$$

[2]As noted in [HS03b, §3.8], the $b=0$ equation is the only member of the b-family that is Galilean invariant.

The traveling fronts $u^0(x)$ cannot be classical solutions of (7), because such solutions must be thrice-differentiable with respect to x, as can be seen from the single equation

$$u_t - u_{xxt} + uu_x - uu_{xxx} = 0, \tag{10}$$

obtained by substituting (7b) into (7a). For the traveling fronts, two ordinary (classical) derivatives u^0_x and u^0_{xx} exist, but the second derivative is discontinuous at $x = 0$, so u^0_{xxx} exists only in the weak sense. Nevertheless, one may verify that $u^0(x)$ satisfies the weak form of (9). Alternatively, one may view $u^0(x)$ as a classical solution of the non-local convective form of the equation given in (5).

Finally, note that the traveling wave solution in the v variable (see (7b)) is given by

$$v^0(x) = \mathcal{H}u^0(x) = \begin{cases} -d & x < 0 \\ d & x > 0. \end{cases} \tag{11}$$

Again, v^0 is a global-in-time weak solution of (7).

Admissible perturbations. As of yet we do not have existence/uniqueness results for weak solutions of (7), so our stability analysis will proceed in a careful way. Let us consider perturbations around the stationary front solutions:

$$u(x,t) = u^0(x) + g(x,t), \tag{12}$$

or equivalently,

$$v(x,t) = v^0(x) + f(x,t), \tag{13}$$

where

$$f = \mathcal{H}g. \tag{14}$$

Unless stated otherwise, we restrict attention to perturbations f such that the perturbed initial data $v(x,0)$ is smooth enough so that the well-posedness theory from [BF] applies. An admissible perturbation $f(x,0)$ is one such that $v(x,0)$ as defined in (13) is continuously differentiable, with two weak derivatives $v_x(x,0)$ and $v_{xx}(x,0)$ in the space $L^1(\mathbb{R})$. In this case, the theory [BF] guarantees the existence of a unique solution $v(x,t)$ globally in time. Note that one implication of this definition is that an admissible perturbation f is going to be initially discontinuous at the origin (as v^0 is discontinuous at $x = 0$ and $v(x,0)$ is smooth).

As boundary conditions at spatial infinity, we take, for all $t \geq 0$:

$$u(-\infty,t) = v(-\infty,t) = -d, \text{ and } u(\infty,t) = v(\infty,t) = d.$$

This yields vanishing at infinity boundary conditions for g and f:

$$g(-\infty,t) = g(\infty,t) = 0, \quad t \geq 0, \tag{15}$$

$$f(-\infty,t) = f(\infty,t) = 0, \quad t \geq 0. \tag{16}$$

Within this admissible class of perturbations, we study the linear, spectral and nonlinear stability of the stationary front solutions u^0 (or v^0). By this we mean precisely that we choose an admissible perturbation $f(x,0)$ (as described above) and study the growth/decay in time of the quantity $\|v(\cdot,t) - v^0(\cdot)\|$ for a suitable choice of norm.

Norms. Let us make two remarks regarding the norms in which we might expect to find stability. By explicitly writing out the convolution (3b) using the kernel (4) with $\alpha = 1$, we obtain

$$u(x,t) = (G * v)(x,t) = \frac{1}{2}\int_{\mathbb{R}} e^{-|x-y|} v(y,t)\, dy. \tag{17}$$

With this equation and Hölder's inequality, we may derive

$$\|u - u^0\|_{L^\infty} \leq \frac{1}{2}\|v - v^0\|_{L^1}. \tag{18}$$

Therefore, L^1 (asymptotic) stability of v^0 yields (asymptotic) stability in the maximum norm for u^0.

In contrast, by defining the characteristics $\eta(X,t)$ as the solution of

$$\begin{aligned} \partial_t \eta(X,t) &= u(\eta(X,t),t) \\ \eta(X,0) &= X, \end{aligned}$$

one finds that (7a) reduces to the statement

$$v(\eta(X,t),t) = v_0(X),$$

implying that the values of v are conserved along characteristics. Thus the initial values $v(x,0)$ are retained in the solution $v(x,t)$ for all $t > 0$, and we cannot hope for asymptotic stability of v^0 in the maximum norm.

3 Linearized Stability

Consider (13), a perturbation about the stationary traveling front solution v^0. After substituting v into the original system (7) and ignoring the quadratic term we find the following linearized equation for the perturbation $f(x,t)$:

$$f_t(x,t) + 2d\delta(x)g(x,t) + u^0(x)f_x(x,t) = 0. \tag{19}$$

Here we used $v_x^0(x) = 2d\delta(x)$. Note that we can write (19) in the form

$$f_t(x,t) = \mathcal{L}f(x,t), \tag{20}$$

where the linear operator $\mathcal{L}$ is defined as

$$\mathcal{L} = -d\left[2\delta(x)\mathcal{H}^{-1} + \bar{u}^0\partial_x\right]. \tag{21}$$

Purely from the form of (21) we may expect the dynamics of (20) to depend significantly on the sign of d.

Using the boundary conditions (16), the linearized stability problem on the real line can be summarized as

$$f_t + 2d\delta(x)g(0,t) + u^0 f_x = 0 \tag{22a}$$

$$f(x,0) = f_0(x) \tag{22b}$$

$$f(-\infty,t) = f(\infty,t) = 0. \tag{22c}$$

We *assume* that (22), with admissible initial data f_0 that is discontinuous at $x = 0$ and smooth elsewhere, possesses a unique global (in time) solution $f(x,t)$. We expect that for $t > 0$, the solution $f(x,t)$ is still discontinuous at $x = 0$ and smooth elsewhere.

3.1 Odd initial data

It turns out that the behavior of (22) can be worked out exactly for *odd* initial data f_0. One can check that if $f(x,t)$ solves the problem (22) with f_0 odd, then $\tilde{f}(x,t) = -f(-x,t)$ solves the same initial value problem with the same initial data. By uniqueness, we must have $f = \tilde{f}$. This implies that odd initial data f_0, evolving forward in time via (22) results in a solution $f(x,t)$ that stays odd for all times.

We could in fact have deduced this from the parity symmetry of (7) mentioned earlier; just note that odd initial data f_0, together with the fact that v^0 is odd, implies by (13) that $v(x,0)$ is odd.

Since $f(x,t)$ is odd for all times, we have

$$g(0,t) = \frac{1}{2}\int_{\mathbb{R}} \exp(-|x|) f(x,t)\, dx = 0, \qquad \text{for } t \geq 0.$$

Hence, the PDE (22a) reduces to the following first-order transport equation with nonconstant speed on the real line:

$$f_t(x,t) + u^0(x) f_x(x,t) = 0. \tag{23}$$

Also note that the values $f(0-,t)$ and $f(0+,t)$ stay constant in time. One obtains this by evaluating the transport equation at $(0-,t)$ and $(0+,t)$ respectively, to get

$$\partial_t f(0\pm,t) = 0.$$

Here we used $u^0(0) = 0$.

The upshot of this is that, for odd initial perturbations $v(x,0)$, we can determine the linear stability of the traveling waves v^0 merely by solving (23) on a half-line only, and then taking the odd extension of the solution.

Proposition 1. *When $d < 0$, the traveling wave v^0 is linearly asymptotically stable with respect to admissible* odd *perturbations $f_0(x)$. When $d > 0$, the traveling wave v^0 is linearly unstable with respect to the same class of perturbations $f_0(x)$.*

Proof. For odd initial data f_0, we solve (23) on the half-line using the method of characteristics; details are given in the Appendix. As discussed above, the odd extension of this half-line solution is the full solution of (23), which we record here:

$$f(x,t) = \begin{cases} f_0\left[-\log\left(1 + \exp(-dt)[\exp(-x) - 1]\right)\right] & x < 0, \\ f_0\left[\log\left(1 + \exp(-dt)[\exp(x) - 1]\right)\right] & x > 0. \end{cases} \tag{24}$$

1. *Case $d < 0$.* As $t \to \infty$, $\exp(-dt) \to +\infty$. For $x < 0$, $[e^{-x} - 1] > 0$. So for arbitrary $x < 0$, we have the limit
$$\lim_{t\to\infty} f(x,t) = \lim_{y\to 0^+} f_0(\log y) = \lim_{x\to-\infty} f_0(x).$$

Because f_0 was chosen such that $f_0(-\infty) = 0$ (see (22c)), we then have, for all $x < 0$,

$$\lim_{t\to\infty} f(x,t) = 0. \tag{25}$$

One can easily check that provided $f_0(+\infty) = 0$, (25) also holds for $x > 0$, implying asymptotic stability.

2. *Case* $d > 0$. As $t \to \infty$, $\exp(-dt) \to 0$ and for arbitrary $x < 0$, we have

$$\lim_{t\to\infty} f(x,t) = \lim_{y\to 1-} f_0(\log y) = f_0(0-).$$

Due to the continuity and the oddness of v, $v(0-,0) = 0$ and hence,

$$f_0(0-) = -v^0(0-) = d.$$

Therefore, for arbitrary $x < 0$,

$$\lim_{t\to\infty} f(x,t) = d.$$

Similarly, for any $x > 0$ fixed,

$$\lim_{t\to\infty} f(x,t) = -d,$$

which shows linear instability.

□

Remarks.

1. The behavior as $t \to \infty$ for a fixed x is very intuitive. For instance, let restrict the attention to the left half-line $x < 0$ only. The variable wave speed $-d + de^x$ is positive for all $x < 0$ if $d < 0$ and negative for all $x < 0$ if $d > 0$. Also, the wave speed vanishes at $x = 0$ and has value $-d$ at $-\infty$. The values of f are propagated along characteristics (see the Appendix) and constrained to satisfy $f(-\infty, t) = 0$ at the left bounday and $f(0-, t) = d$ at the right boundary. For $x < 0$ fixed and $d < 0$ (positive wave speed) when taking $t \to \infty$ we obtain 0 (the value progagated from $-\infty$). We will see later that we can prove a version of this statement in the fully nonlinear setting. Similarly, for $d > 0$ (negative wave speed), as $t \to \infty$ we will obtain d (the value progagated from 0).

2. Generally speaking, when we analyze stability/instability of equilibrium solutions for nonlinear PDE's, we should not dwell on linearized results by themselves, since these results are neither necessary nor sufficient for the corresponding nonlinear stability/instability results. However, for both $d > 0$ and $d < 0$ cases, the above linearized results seem to correspond rather well to the fully nonlinear picture.

3.2 Arbitrary initial data

We now turn to linear stability with respect to arbitrary admissible perturbations f_0. Let us remind the reader that we have assumed well-posedness of (22) in a function space where $f(x,t)$ is discontinuous at $x=0$ but smooth elsewhere. In this case, we can prove

Proposition 2. *When $d<0$, the traveling wave v^0 is linearly stable in the L^1 norm, with respect to any admissible perturbation f_0, i.e., any f_0 such that*

$$v(x,0) = v^0(x) + f_0(x)$$

is smooth.

Proof. Multiply the equation (22a) by $\operatorname{sgn}(f(x,t))$ and integrate over $(-\infty,+\infty)$. We obtain

$$\frac{d}{dt}\int_{-\infty}^{\infty} |f(x,t)|\,dx + \int_{-\infty}^{0} \left(-d+de^{x}\right)|f(x,t)|_x\,dx + \int_{0}^{\infty}\left(d-de^{-x}\right)|f(x,t)|_x\,dx + 2d\int_{-\infty}^{\infty}\delta(x)g(x,t)\operatorname{sgn}(f(x,t))\,dx = 0. \quad (26)$$

First we integrate by parts the second integral on the left-hand side of (26), obtaining

$$\begin{aligned}\int_{-\infty}^{0}\left(-d+de^{x}\right)|f(x,t)|_x\,dx &= \int_{-\infty}^{0}\left[\left(-d+de^{x}\right)|f(x,t)|\right]_x - \int_{-\infty}^{0} de^{x}|f(x,t)|\,dx\\ &= -d\int_{-\infty}^{0} e^{x}|f(x,t)|\,dx.\end{aligned}$$

To write the last equality, we used: $f(-\infty,t)=0$ and $-d+de^{x}\,|_{x=0}=0$. Integrating by parts the third integral on the left-hand side of (26) results in

$$\int_{0}^{\infty}\left(d-de^{-x}\right)|f(x,t)|_x\,dx = -d\int_{0}^{\infty} e^{-x}|f(x,t)|\,dx.$$

The only remaining term on the left-hand side of (26) can be evaluated using properties[3] of the δ distribution:

$$2d\int_{-\infty}^{\infty}\delta(x)g(x,t)\operatorname{sgn}(f(x,t))\,dx = 2dg(0,t)\frac{1}{2}\left[\operatorname{sgn}(f(0-,t))+\operatorname{sgn}(f(0+,t))\right].$$

[3] As shown in [Kur96], the distribution $\delta(x)$ can be applied to a function $\Phi(x)$ that is discontinuous at 0 with the result

$$\frac{1}{2}\left[\Phi(0-)+\Phi(0+)\right].$$

Roughly speaking, $\delta(x)$ is the weak limit $a\to 0$ of the function $\frac{1}{2a}1_{[-a,a]}$, where 1_A represents the characteristic function of the set A. Now, for Φ discontinuous,

$$\begin{aligned}\langle\delta,\Phi\rangle &= \lim_{a\to 0}\frac{1}{2a}\int_{-a}^{a}\Phi(x)\,dx\\ &= \lim_{a\to 0}\frac{1}{2a}\left(\int_{-a}^{0}\Phi(x)\,dx+\int_{0}^{a}\Phi(x)\,dx\right)\\ &= \frac{1}{2}\left[\Phi(0-)+\Phi(0+)\right].\end{aligned}$$

Gathering all the results, we may rewrite (26):

$$\frac{d}{dt}\int_{-\infty}^{\infty}|f(x,t)|\,dx = d\left(\int_{-\infty}^{\infty}e^{-|x|}|f(x,t)|\,dx - g(0,t)\left[\operatorname{sgn}(f(0-,t))+\operatorname{sgn}(f(0+,t))\right]\right).$$

Using

$$g(0,t) = \frac{1}{2}\int_{-\infty}^{\infty}e^{-|x|}f(x,t)\,dx,$$

we may estimate

$$g(0,t)\left[\operatorname{sgn}(f(0-,t))+\operatorname{sgn}(f(0+,t))\right] \le \int_{-\infty}^{\infty}e^{-|x|}|f(x,t)|\,dx.$$

Hence,

$$\frac{d}{dt}\int_{-\infty}^{\infty}|f(x,t)|\,dx = dM,$$

with $M \ge 0$. This gives

$$\frac{d}{dt}\int_{-\infty}^{\infty}|f(x,t)|\,dx \le 0,$$

when $d < 0$. Therefore, for any $\epsilon > 0$, we may choose any admissible f_0 such that $\|f_0\|_{L^1} < \epsilon$. The above calculation shows that for all $t > 0$,

$$\|f(\cdot,t)\|_{L^1} \le \|f_0\|_{L^1} < \epsilon.$$

□

Corollary 1. *Using (18), we conclude that for $d < 0$, linear stability of v^0 in the L^1 norm implies linear stability of u^0 in the maximum norm. The stability of u^0 is with respect to perturbations g^0 such that $f^0 = \mathcal{H}g^0$ is admissible.*

3.3 Spectral Instability

To show instability of the linearized problem in the $d > 0$ case, we solve the eigenvalue problem

$$\mathcal{L}f = \lambda f,$$

with $\mathcal{L}$ defined in (21). We show that when $d > 0$, there exist eigenvalue-eigenfunction pairs (λ, f_λ) such that λ has positive real part and $f_\lambda \in L^1(\mathbb{R})$. To see that this implies linear instability, consider linearized dynamics along an unstable eigenfunction, i.e., consider (22) with initial data

$$f_0(x) = Kf_\lambda(x).$$

By choosing K, we can make $\|f_0\|_{L^1}$ as small as we wish. The solution of (20) with initial data f_0 is then given by

$$f(x,t) = Kf_\lambda(x)e^{\lambda t},$$

and because λ has positive real part, $\|f(\cdot,t)\|_{L^1} \to \infty$ as $t \to \infty$.

We begin with the following:

Definition 1. *By a real solution f of the eigenvalue problem $\mathcal{L}f = \lambda f$, we mean a function $f : \mathbb{R} \to \mathbb{R}$ such that*

- *For $x \neq 0$, f satisfies the pointwise equality*

$$-d\bar{u}^0(x)f'(x) = \lambda f(x). \tag{27}$$

- *For $\epsilon > 0$ sufficiently small, f satisfies the jump condition*

$$-d\int_{-\epsilon}^{\epsilon} \left[2\delta(x)\left(\mathcal{H}^{-1}f\right)(x) + \bar{u}^0(x)f'(x)\right] dx = \lambda\int_{-\epsilon}^{\epsilon} f(x). \tag{28}$$

An L^1 eigenfunction of $\mathcal{L}$ is a solution in the above sense that also satisfies $f \in L^1(\mathbb{R})$.

With this definition, we note the following remarkable fact:

Lemma 1. *Any odd function $f \in L^1$ automatically satisfies the jump condition (28) in Definition 1, for any $0 < \epsilon \leq \infty$.*

Proof. Fix $\epsilon > 0$. Because f is odd, the right-hand side of (28) is zero. Similarly, the integral of the second term in the left-hand side of (28) vanishes due to the fact that the integrand is odd ($\bar{u}^0$ is odd and f' is even, so their product is odd). As regards the integral of the first term in the left-hand side of (28), this can be evaluated as follows:

$$\begin{aligned} -d\int_{-\epsilon}^{\epsilon} 2\delta(x)\left(\mathcal{H}^{-1}f\right)(x)\,dx &= -2d\left(\mathcal{H}^{-1}f\right)(0) \\ &= -2d\int_{-\infty}^{\infty} G(x)f(x)\,dx. \end{aligned}$$

The last integral is also zero as the integrand is odd (G is even and f is odd).

Hence, for any f odd, the jump condition (28) is automatically satisfied. Note that $f \in L^1$ implies that we could have taken $\epsilon = \infty$ and all relevant integrals exist, so the lemma holds. □

With this lemma in mind, we solve (27) for an odd, real function $f \in L^1$. The steps involved in the solution are entirely elementary, so we skip ahead to the eigenfunctions, given below:

Proposition 3. *For any $d \neq 0$, the function*

$$f(x) = \frac{\operatorname{sgn} x}{(-1 + e^{|x|})^{\sigma}}, \qquad \text{with } 0 < \sigma < 1, \tag{29}$$

is an L^1 eigenfunction of $\mathcal{L}$ with eigenvalue $\lambda = \sigma d$.

Proof. We need to check that (29) satisfies (27), (28) and that $f \in L^1$.

For $x > 0$,

$$\frac{f(x)}{f'(x)} = -\frac{1}{\sigma}\left(-1 + e^{x}\right)e^{-x} = -\frac{1}{\sigma}\bar{u}^0.$$

Similarly, for $x < 0$,

$$\frac{f(x)}{f'(x)} = -\frac{1}{\sigma}\left(1 - e^{-x}\right)e^{x} = -\frac{1}{\sigma}\bar{u}^0.$$

Hence for $\sigma = \lambda/d$, the equation (27) is satisfied for all $x \neq 0$.

Because f as defined in (29) is an odd, real function, we use Lemma 1 to conclude that the jump condition (28) is automatically satisfied. Therefore, f solves the eigenvalue problem $\mathcal{L}f = \lambda f$ with eigenvalue $\lambda = \sigma d$.

Next we show that $0 < \sigma < 1$ implies $f \in L^1(\mathbb{R})$. Making the substitutions $x = \log\phi$, $y = \phi - 1$, and $a = 1 - \sigma$, we obtain

$$\int_0^\infty \frac{dx}{(-1+e^x)^\sigma} = \int_1^\infty \frac{d\phi}{\phi(\phi-1)^\sigma} = \int_0^\infty \frac{y^{a-1}}{y+1}\,dy = \pi\csc\sigma\pi. \tag{30}$$

The last equality is valid only for $0 < a < 1$, and can be derived via contour integration[4]. Symmetry of $|f|$ then implies that

$$\|f\|_{L^1} = 2\pi\csc\sigma\pi.$$

□

Remarks.

1. It is now clear that for $d > 0$, there exist real, odd L^1 eigenfunctions (29). Moreover, the eigenvalues associated to these eigenfunctions, when $d > 0$, are given by $\lambda = \sigma d > 0$. This means that the $d > 0$ traveling waves v^0 are linearly unstable in L^1.

2. The same calculation shows that if we seek $f \in L^1(\mathbb{R}) \cap L^p(\mathbb{R})$, with $p > 1$, we simply choose σ such that $0 < \sigma < 1/p$. This says that the $d > 0$ traveling waves v^0 are linearly unstable in every L^p norm for $1 \leq p < \infty$.

4 Nonlinear stability

In the previous section we showed that if d is negative (respectively, positive), then the equilibrium is linearly stable (respectively, unstable) with respect to admissible perturbations. One strategy would be to attempt to extend these results on the linearized equation (20) to the fully nonlinear equation

$$f_t = \mathcal{L}f - \epsilon\left(\mathcal{H}^{-1}f\right)f_x,$$

which is what one obtains by substituting $v = v^0 + \epsilon f$ into (7a). We emphasize that this is *not* the path pursued here.

Instead, we work with (7) directly and make heavy use of the characteristic form of equation (7a). We will show that for the $d < 0$ waves, if the perturbed initial data is strictly decreasing and odd, then the solution must tend towards the traveling wave exact solution, asymptotically in time.

[4]This particular integration is explained in many complex analysis texts—see, for example, Titchmarsh's *The Theory of Functions*, 1939, computation 3.123 on pp. 105-106.

Characteristics. Let us briefly review[5] some of the theory regarding characteristics of (7). We first define the characteristic curves $\eta(X,t)$ as solutions of

$$\partial_t \eta(X,t) = u(\eta(X,t),t) \tag{31a}$$

$$\eta(X,0) = X. \tag{31b}$$

Hence (7a) evaluated at $x = \eta(X,t)$ can be rewritten as

$$\frac{d}{dt}\left[v(\eta(X,t),t)\right] = 0,$$

implying

$$v(\eta(X,t),t) = v_0(X), \tag{32}$$

for all X and t. We assume that

$$v_0 \in C^1(\mathbb{R}) \quad \text{and} \quad v_0', v_0'' \in L^1(\mathbb{R}). \tag{33}$$

Then by results in [BF], a unique solution $v(\cdot,t)$ exists globally in time and retains its initial smoothness. We may differentiate both sides of (32) to obtain

$$v_x(\eta(X,t),t)\eta_X(X,t) = v_0'(X). \tag{34}$$

Because $u(\cdot,t) = \mathcal{H}^{-1}v(\cdot,t) \in C^2(\mathbb{R})$, and because η solves (31a), the existence and uniqueness theorem for ODE's implies that $\eta(\cdot,t) \in C^2(\mathbb{R})$ for all $t \geq 0$.

Asymptotic Stability. The main result of this section is contained in the following theorem. The idea behind the theorem is to restrict attention to odd and strictly decreasing initial data v_0. In this case, we can show through the method of characteristics and local analysis that $v(x,t)$, $u(x,t)$, $u_x(x,t)$, $\eta(X,t)$, and $\partial_t\eta(X,t)$ must all converge pointwise in x as $t \to \infty$. Note that if η and $\partial_t\eta$ are both converging as $t \to \infty$, then $\partial_t\eta$ must converge pointwise to zero—no other limit is possible. By using formula (31a), we then arrive at the following dichotomy: either

- $\eta(X,t)$ converges pointwise to zero, or
- $u_x(0,t)$ converges to zero.

At this stage, we are able to employ the non-local form of the PDE to relate the asymptotic behavior of $u_x(0,t)$ to the asymptotic behavior of $\eta(X,t)$ for almost all X. Specifically, we show that $\eta(X,t)$ converges pointwise in X to a bounded function, as $t \to \infty$. Then by the formula (derived in the proof below),

$$u_x(0,t) = \frac{1}{2}\int_{-\infty}^{\infty} e^{-|\eta(X,t)|} v_0'(X)\, dX < 0,$$

it is impossible for $u_x(0,t)$ to converge to zero. Only the first case of the above dichotomy is possible, implying that $\eta^{-1}(x,t)$ diverges pointwise to $\operatorname{sgn}(x)\cdot\infty$. By the formula

$$v(x,t) = v_0\left(\eta^{-1}(x,t)\right),$$

[5]For more details, see [BF].

this tells us that $v(\cdot,t)$ approaches the exact solution v^0, pointwise in x and asymptotically as $t \to \infty$. We believe this technique of using the non-locality of the PDE to go from local to global asymptotics may yield interesting results in the future.

Theorem 1. *Suppose that v_0 satisfies (33) and is odd and strictly decreasing ($v_0' < 0$), with boundary values $v_0(\pm\infty) = \pm d$ where $d < 0$. Then, as $t \to \infty$, the solution $v(x,t)$ converges (pointwise in x) to the traveling wave solution (11), $v^0(x) = d\,\mathrm{sgn}(x)$.*

Proof. The proof proceeds in several stages.

Claim 1: The solution stays odd for all $t > 0$. In the Introduction, we mentioned that odd initial data $u(x,0)$ for (7) results in a solution $u(x,t)$ that is odd for all t. Note that $u(x,t)$ is an odd function of x if and only if $v(x,t)$ is an odd function of x. The forward direction is easy: if u is odd, then u_x is even, and u_{xx} is odd. Hence $v = u - u_{xx}$ must be odd. To show the reverse direction we use $u = G * v$. Assuming that v is odd then u is also odd as a convolution of an even and an odd function (the kernel G is even).

Therefore, taking v_0 to be odd guarantees that both $u(x,t)$ and $v(x,t)$ are odd for all $t \geq 0$.

Claim 2: For all $t > 0$, we have $\eta_X > 0$, $v_x < 0$, and $u_x < 0$. Initially we have $\eta_X(X,0) = 1$. Suppose there exists (X_0, t_0) such that $\eta_X(X_0,t_0) = 0$. The regularity theory [BF] guarantees that the characteristics do not cross in finite time, which implies $v_x(\eta(X_0,t_0),t_0) < \infty$. Then it is clear from (34) that $v_0'(X_0) = 0$, a contradiction. Therefore $\eta_X > 0$ for all $t > 0$. We may rewrite (34) as

$$v_x(x,t) = \frac{v_0'(\eta^{-1}(x,t))}{\eta_X(\eta^{-1}(x,t),t)},$$

and it is clear that $v_x < 0$ for all $t > 0$. Then $u_x = G * v_x$ implies that $u_x < 0$ for all $t > 0$.

Claim 3: At every $t > 0$, $\eta(X,t)$ is an odd diffeomorphism of $\mathbb{R}$ onto itself. Since $v_x < 0$, for each t, $v(\cdot,t)$ is a diffeomorphism of $\mathbb{R}$ onto the open interval $(d,-d)$ where $d < 0$. Hence we may invert (32) and write $\eta(X,t) = v^{-1}(v_0(X),t)$. Using *Claim 1* we infer that v^{-1} is odd (as the inverse of an odd function). Then, η is odd (as the composition of two odd functions).

Now consider (32) for an arbitrary $t > 0$. Clearly the right-hand side of (32) has the limits $\pm d$ as $X \to \pm\infty$. Therefore,

$$\lim_{X\to\pm\infty} v(\eta(X,t),t) = \pm d.$$

Let us put together (i) the boundary conditions on v, (ii) the fact that v is one-to-one for all t, and (iii) the fact that $\eta_X > 0$ always. Based on these three facts, we conclude that

$$\lim_{X\to\pm\infty} \eta(X,t) = \pm\infty.$$

Claim 4: $\eta(X,t)$ converges, pointwise in X, as $t \to \infty$. Because η is odd, we have $\eta(0,t) = 0$. Since $\eta_X > 0$ always, we have $\eta(X,t) > 0$ for $X > 0$. Because $u_x < 0$ always, we know $u(x,t) < 0$ for $x > 0$. Putting these facts together inside (31a), we conclude that $X > 0$ implies

$$\partial_t \eta(X,t) = u(\eta(X,t),t) < 0.$$

For each $X > 0$, $\eta(X,t)$ is a bounded monotone sequence in t, and hence must converge as $t \to \infty$ to some finite limit which we denote by $\bar{\eta}(X)$, i.e.

$$\bar{\eta}(X) = \lim_{t\to\infty} \eta(X,t). \tag{35}$$

Claim 5: $v(x,t)$ converges pointwise as $t \to \infty$ to a monotone function. For all $t > 0$ and $x > 0$, we have the bounds (with $d < 0$)

$$d < u(x,t) < 0,$$
$$d < v(x,t) < 0.$$

Note that

$$v_t(x,t) = -u(x,t)v_x(x,t) < 0,$$

so again for each x, $v(x,t)$ is a bounded monotone sequence in t, and therefore must converge to some finite limit which we label as $\bar{v}(x)$. Note in particular that we have the estimates, for all $t > 0$,

$$x > 0 \;\Rightarrow\; 0 > v(x,t) > \bar{v}(x) \geq d$$
$$x < 0 \;\Rightarrow\; 0 < v(x,t) < \bar{v}(x) \leq -d.$$

It is obvious upon taking the appropriate limits that (with $d < 0$)

$$\lim_{x\to\pm\infty} \bar{v}(x) = \pm d.$$

Furthermore, because for each finite $t > 0$, we have $v_x(x,t) < 0$, it is clear that $\bar{v}$ is monotonic, i.e.,

$$x < y \;\Rightarrow\; \bar{v}(x) \geq \bar{v}(y).$$

Any bounded monotonic function has finite total variation, so $\bar{v} \in BV(\mathbb{R})$, and therefore[6] $\bar{v}$ is differentiable almost everywhere, and discontinuous at most on a countable subset of $\mathbb{R}$.

Claim 6: $u(x,t)$ and $u_x(x,t)$ converge, pointwise in x, as $t \to \infty$. Fix $x, y \in \mathbb{R}$. Then note that pointwise convergence of $v(y,t) \to \bar{v}(y)$ implies pointwise convergence:

$$G(x-y)v(y,t) \to G(x-y)\bar{v}(y).$$

Moreover this sequence is bounded uniformly in t by an integrable function:

$$|G(x-y)v(y,t)| \leq |d|G(x-y).$$

Then by Lebesgue's dominated convergence theorem, we know that $G * v \to G * \bar{v}$ as $t \to \infty$, implying pointwise convergence of $u(x,t)$. Let us denote

$$\bar{u}(x) = \lim_{t\to\infty} u(x,t) = (G * \bar{v})(x). \tag{36}$$

[6]See Folland, *Real Analysis*, Theorems 3.23 and 3.27.

It is clear from the properties of $\bar{v}$ established above that $\bar{u}$ is everywhere differentiable.

For $u_x(x,t)$, we use $u_x = G * v_x = G' * v$. As G' is integrable, the same arguments as above work to obtain

$$\begin{aligned}\lim_{t\to\infty} u_x(x,t) &= \left(G' * \bar{v}\right)(x) \\ &= \bar{u}'(x). \end{aligned} \tag{37}$$

Claim 7: $\partial_t\eta(X,t)$ converges to zero, pointwise in X, as $t \to \infty$. First note that

$$\lim_{t\to\infty} u(\eta(X,t),t) = \bar{u}(\bar{\eta}(X)). \tag{38}$$

Equation (38) follows from

$$\begin{aligned}|u(\eta(X,t),t) - \bar{u}(\bar{\eta}(X))| &\le |u(\eta(X,t),t) - u(\bar{\eta}(X),t)| + |u(\bar{\eta}(X),t) - \bar{u}(\bar{\eta}(X))| \\ &\le \|u_x\|_{L^\infty}|\eta(X,t) - \bar{\eta}(X)| + |u(\bar{\eta}(X),t) - \bar{u}(\bar{\eta}(X))|,\end{aligned}$$

where one uses (35), (36) and the uniform estimate:

$$\|u_x\|_{L^\infty} \le \|G_x\|_{L^1}\|v\|_{L^\infty} = \|v_0\|_{L^\infty}.$$

The last equality above comes from the characteristic form of the equation (7a) (the values of v are conserved along characteristics).

Now, from (31a) and (38) we conclude that $\partial_t\eta(X,t)$ must convergence pointwise as $t \to \infty$. Since $\eta(X,t)$ is also converging (and is bounded), the only possible limit value is, for all X,

$$\lim_{t\to\infty} \partial_t\eta(X,t) = 0.$$

Also, from (31a),

$$\lim_{t\to\infty} u(\eta(X,t),t) = 0. \tag{39}$$

Claim 8: $\eta(X,t)$ converges to zero, pointwise in X, as $t \to \infty$. We will prove this claim by contradiction. Suppose that there exists some $Y > 0$ such that $\lim_{t\to\infty}\eta(Y,t) = P > 0$. We have

$$|u(\eta(Y,t),t) - u(P,t)| \le \|u_x\|_{L^\infty}|\eta(Y,t) - P|,$$

which together with (39) and the observation about the uniform bound on $\|u_x\|_{L^\infty}$, yields

$$\lim_{t\to\infty} u(P,t) = 0.$$

Because for each $t > 0$, the function $u(x,t)$ is a strictly decreasing and odd function of x, we see that for $x \in [-P,P]$, we must have

$$\bar{u}(x) = \lim_{t\to\infty} u(x,t) = 0.$$

Therefore, by using (37) we get

$$\lim_{t\to\infty} u_x(0,t) = 0. \tag{40}$$

Consider

$$u_x(0,t) = \frac{1}{2}\int_{-\infty}^{\infty} e^{-|y|} v_y(y,t)\, dy.$$

Because η is a diffeomorphism of $\mathbb{R}$ onto itself (see *Claim 3*), we can make the change of variables $y = \eta(X,t)$, and obtain the equivalent integral

$$u_x(0,t) = \frac{1}{2}\int_{-\infty}^{\infty} e^{-|\eta(X,t)|} v_y(\eta(X,t),t)\eta_X(X,t)\, dX.$$

Using (34), we have

$$u_x(0,t) = \frac{1}{2}\int_{-\infty}^{\infty} e^{-|\eta(X,t)|} v_0'(X)\, dX < 0, \quad \text{for all } t\ . \tag{41}$$

By (40), we must have, for almost every X,

$$|\eta(X,t)| \to +\infty, \qquad \text{as } t \to \infty,$$

contradicting the boundedness of η (see *Claim 4*). Therefore, for all $Y > 0$,

$$\lim_{t\to\infty} \eta(Y,t) = 0.$$

By oddness of η, the claim is established.

Claim 9: $v(x,t)$ converges pointwise to the traveling wave solution (11), determined completely by the boundary data of v_0. Since η converges to zero, it is clear by reflecting η across the line $Y = X$ that η^{-1} must diverge to $\pm\infty$, i.e.,

$$\lim_{t\to\infty} \eta^{-1}(x,t) = \begin{cases} +\infty & x > 0 \\ -\infty & x < 0. \end{cases}$$

Therefore,

$$\lim_{t\to\infty} v(x,t) = \lim_{t\to\infty} v_0(\eta^{-1}(x,t)) = \begin{cases} d & x > 0 \\ -d & x < 0, \end{cases}$$

proving the theorem.

□

5 Numerical results

We solve numerically (7) by using a hybrid Lagrangian/Eulerian scheme. Below we briefly describe the numerical scheme and then discuss various numerical results regarding the nonlinear stability/ instability of the traveling waves for both $d < 0$ and $d > 0$ cases.

Numerical scheme. We are interested in solving (7) with initial data

$$v(x,0) = v_0(x),$$

and boundary conditions

$$v(-\infty,t) = -d, \text{ and } v(\infty,t) = d, \text{ for all times } t.$$

Solving this initial boundary value problem for (7) is equivalent to computing the Lagrangian map η, as defined by (31), and then setting

$$v(\eta(X,t),t) = v_0(X). \tag{42}$$

Here, X denotes the generic Lagrangian variable (the particle label), while x represents the Eulerian variable.

For numerical purposes we truncate the spatial domain to $[-a,a]$, with a large enough, and impose artificial boundary conditions: $v(x,t) = -d$ for $x < -a$ and $v(x,t) = d$ for $x > a$. We discretize the domain $[-a,a]$ using an equispaced grid with N grid points. Let us denote this grid by $x_i = -a + (i-1)\Delta x$, where $i = 1,\dots,N$, and the grid spacing is given by $\Delta x = 2a/(N-1)$. We consider N "particles" X_i located initially at x_i, $i = 1,\dots,N$. We store the initial values $v_0(X_i)$ in a vector $\mathbf{v_0}$; these values will be preserved along the characteristics originating from X_i, $i = 1,\dots,N$. To update the solution in time we use a fixed timestep Δt and a sequence of discrete times $t_n = n\Delta t$.

Let $\mathbf{x} = (x_1,\dots,x_N)$ and $\mathbf{X} = (X_1,\dots,X_N)$. We track numerically the positions of the particles X_i at the discrete times t_n, i.e., we compute $\eta^n(\mathbf{X}) = (\eta^n(X_1),\dots,\eta^n(X_N))$, where $\eta^n(X_i) \approx \eta(X_i,t_n)$, $i = 1,\dots,N$. On the Eulerian grid we compute $\mathbf{v}^n = (v_1^n,\dots,v_N^n)$, where $v_i^n \approx v(x_i,t_n)$, $i = 1,\dots,N$. Analogously, $\mathbf{u}^n$ denotes the numerical approximation on the discrete spacetime grid of $u(x,t)$.

We will write down step n of the algorithm, which presupposes that we have computed $\eta^{n-1}(\mathbf{X})$, $\mathbf{v}^{n-1}$ and $\mathbf{u}^{n-1}$.

1. Step forward one unit of time Δt, from $\eta^{n-1}(\mathbf{X})$ to $\eta^n(\mathbf{X})$, using the evolution equation (31a). Numerically, we have a vector $\mathbf{u}^{n-1}$ which tells us u evaluated at each of the Eulerian grid points x_i, $i = 1,\dots,N$. We can interpolate these values at $\eta^{n-1}(\mathbf{X})$ and use the forward Euler method [7] for (31a) to step forward in time and compute $\eta^n(\mathbf{X})$.

2. Due to (42), we know the numerical values of v at $\eta^n(\mathbf{X})$; these are given by $\mathbf{v_0}$, as they have been preserved along the characteristics. We interpolate these values at $\mathbf{x}$ to compute $\mathbf{v}^n$.

3. Invert numerically the Helmholtz operator on the Eulerian grid and compute $\mathbf{u}^n$ from $\mathbf{v}^n$ (see details below).

[7] Of course, we could use a much better time-stepper than forward Euler. To generate the numerical results presented in this section we used standard Runge-Kutta methods.

Let us describe briefly how we invert numerically the Helmholtz operator $\mathcal{H}$, as needed in step 3 of the algorithm. Define the following operator on $\mathbb{R}^N$:

$$\mathbf{z} \mapsto \Delta_0^2 \mathbf{z}, \quad \left(\Delta_0^2 \mathbf{z}\right)_k = z_{k+1} - 2z_k + z_{k-1}. \tag{43}$$

Here we use the convention that $z_k = -d$ for $k < 1$ and $z_k = d$ for $k > N$. This corresponds to the artificial boundary conditions discussed above. The operator (43) is a linear transformation of $\mathbb{R}^N$ and may be written in matrix form. Now consider the following standard finite-difference approximation to the second-derivative operator ∂_x^2 (see [Ise96]):

$$D^2 = \frac{1}{\Delta x^2}\left[\left(\Delta_0^2\right) - \frac{1}{12}\left(\Delta_0^2\right)^2 + \frac{1}{90}\left(\Delta_0^2\right)^3\right] + \mathcal{O}(\Delta x^6). \tag{44}$$

With this notation, the discrete form of $u = \mathcal{H}^{-1} v$ reads

$$\mathbf{u} = \left(\mathrm{Id} - \alpha^2 D^2\right)^{-1} \mathbf{v}.$$

Remark. As usual with Lagrangian methods, we need to perform regridding after a certain number of timesteps. Otherwise, the particles tend to cluster together and/or move away from each other. In the examples presented in Figures 1 and 3-5, for instance, the particles will cluster in a very narrow region where the shock forms.

Odd initial data. In Section 4, we showed the nonlinear asymptotic stability with respect to strictly decreasing odd perturbations of the traveling wave solution for $d < 0$. We present below a numerical test that confirms this analytical result. We also consider the $d > 0$ case and take perturbed initial states that are odd and strictly increasing. The numerical results in the latter case indicate that the $d > 0$ waves are nonlinearly unstable, as suggested by the analytical results on the linearized problem from Section 3.3.

We take as initial data,

$$v_0(x) = d \tanh\left(\frac{x}{w}\right), \tag{45}$$

with $d = -1$, $d = 1$ and $w = 4$, $w = 0.5$, respectively. The numerical results are presented in Figures 1 and 2. For $d < 0$ (see Figure 1), the numerics confirm that the traveling waves are asymptotically stable with respect to perturbations resulting from odd, strictly decreasing perturbed initial states v_0. Table 1 shows how $\|v(\cdot,t) - v^0(\cdot)\|_{L^1}$ and $\|u(\cdot,t) - u^0(\cdot)\|_{L^\infty}$ decay over time. For $d > 0$ (see Figure 2) the numerics suggest that the traveling waves are nonlinearly unstable.

We also experimented with other odd initial data for $d < 0$. The numerical results indicate that the traveling waves v^0 are asymptotically stable in the L^1 norm. We considered for instance:

$$v_0(x) = -\tanh\left(\frac{x}{w_1}\right) - 2\frac{x/w_2}{(x/w_2)^6 + 1}, \tag{46}$$

with $w_1 = 3$ and $w_2 = 4$. The numerical results for initial data (46) are presented in Figure 3.

Remark. Note that for $d < 0$, the odd initial perturbations (45) and (46) that we considered are quite large, yet we still get numerical evidence of nonlinear asymptotic stability, which is quite remarkable.

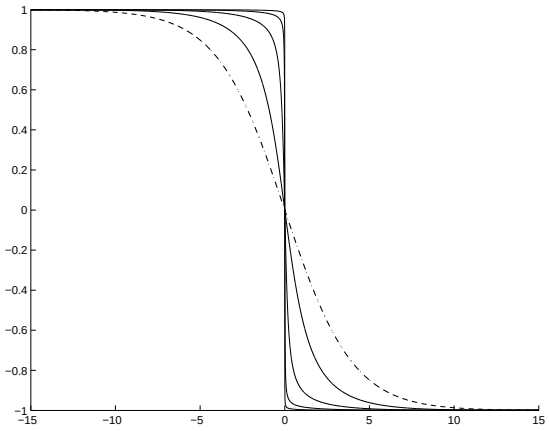

Figure 1: Case $d = -1 < 0$ (asymptotic stability). The initial profile (45) (dash-dot line) will approach the traveling wave solution v^0 (see (11)) as $t \to \infty$. The solid lines represent the solution at $t = 3$, 6, 9, 12, respectively. See also Table 1.

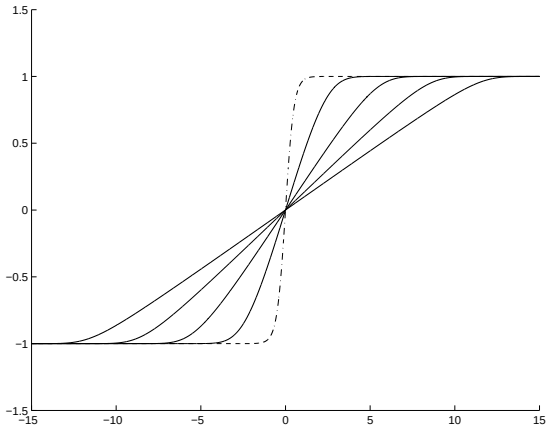

Figure 2: Case $d = 1 > 0$ (instability). The initial profile (45) (dash-dot line) "rarefacts", i.e. approaches, as $t \to \infty$, a line that connects the left and right states $u_L = -1$, $u_R = 1$ at $-\infty$ and ∞, respectively. The solid lines represent the solution at $t = 3$, 6, 9, 12, respectively.

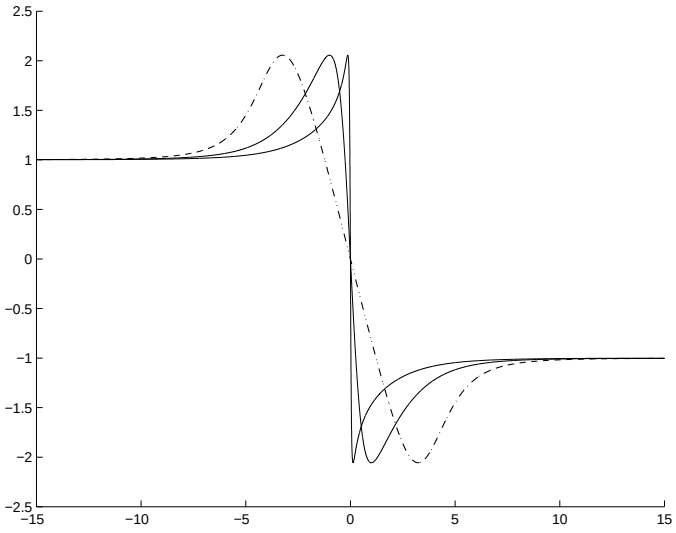

Figure 3: Numerical results for $d = -1$ and the initial data given by (46). The initial profile (dash-dot line) approaches the traveling wave solution v^0 a.e. as $t \to \infty$. The solid lines represent the solution at $t = 1.5$ and 3. Numerical experiments with higher resolution confirm that the widths of the two symmetric bumps will become infinitesimally small, while the bumps keep constant values at their peaks.

Table 1: The decay over time of the L^1 norm $\|v(\cdot,t) - v^0(\cdot)\|_{L^1}$ and the L^∞ norm $\|u(\cdot,t) - u^0(\cdot)\|_{L^\infty}$. Here, v (and u) represent the numerical solution corresponding to the initial data (45) with $d = -1$. Computations using higher resolution and larger times confirm the decay to 0 of the two norms as $t \to \infty$. See also Figure 1.

Time	$\|v - v^0\|_{L^1}$	$\|u - u^0\|_{L^\infty}$
0	5.5408	0.4489
3	2.8500	0.2434
6	0.9015	0.0618
9	0.1801	0.0108
12	0.0338	0.0022
15	0.0054	4.2×10^{-4}
18	3.6×10^{-4}	7.6×10^{-6}

Other initial data for the $d < 0$ case. Inspired by the extensive prior work on the stability of viscous profiles [Sat76, Goo86], we expect that the stationary traveling waves should be at best "orbitally stable", that is, if $v(x,0) \approx v^0(x)$, then $v(x,t) \to v^0(x + x_0)$ as $t \to \infty$, where x_0 is some constant shift. To see this more clearly, take a perturbation around a steady traveling wave,

$$v(x,t) = v^0(x) + f(x,t),$$

where $v(x,t)$ is a solution of (7). One can check that

$$\frac{d}{dt}\int_{\mathbb{R}} f(x,t)\,dx = 0,$$

which implies that for all t, we have

$$\int_{\mathbb{R}} f(x,t)dx = \int_{\mathbb{R}} f(x,0)\,dx.$$

Suppose that we have orbital stability, i.e.,

$$v(x,t) \to v^0(x + x_0), \text{ as } t \to \infty.$$

Then

$$\int_{\mathbb{R}} (v^0(x + x_0) - v^0(x))\,dx = \int_{\mathbb{R}} f(x,0)\,dx.$$

Denote[8]

$$\Psi(x_0) = \int_{\mathbb{R}} (v^0(x + x_0) - v^0(x))\,dx.$$

We have $\Psi(0) = 0$ and

$$\Psi'(x_0) = \int_{\mathbb{R}} (v^0)'(x + x_0)\,dx = 2d.$$

[8]We would like to thank Tai-Ping Liu for showing us this trick.

Hence,

$$\Psi(x_0) = 2dx_0,$$

and

$$x_0 = \frac{1}{2d}\int_{\mathbb{R}} f(x,0)\,dx. \tag{47}$$

Therefore, provided we have orbital stability, the shift x_0 is determined entirely by the initial perturbation $f(x,0)$ at $t=0$, and by the value of d.

Our next step is to present numerical tests of orbital stability that take into account (47). We considered the following two choices of non-odd initial data ($d=-1$):

$$v_0(x) = -\tanh\left(\frac{x}{w_1}\right) + 0.2\left(2\left(x/w_2\right)^2 - 1\right)\exp\left(-\left(x/w_2\right)^2\right), \tag{48}$$

and

$$v_0(x) = -\tanh\left(\frac{x}{w_1}\right) + \frac{0.2}{(x/w_2)^4+1}, \tag{49}$$

with $w_1 = 1$ and $w_2 = 2$.

The initial data given by (48) has zero integral, i.e. $\int_{-\infty}^{\infty} v_0(x)\,dx = 0$ and hence we are interested in checking numerically if this profile approaches, as $t\to\infty$, the unshifted traveling wave $v^0(x)$.

On the other hand, the initial data given by (49) has a non-zero integral; in this case, we check numerically whether the profile approaches, as $t\to\infty$, a shifted traveling wave $v^0(x+x_0)$. The shift x_0 can be computed using (47)—for the initial data (49), we have $x_0 \approx -0.4443$.

The numerical results for initial data (48) and (49) are presented in Figures 4-6. Tables 2 and 3 show how $\|v(\cdot,t) - v^0(\cdot)\|_{L^1}$ and $\|u(\cdot,t) - u^0(\cdot)\|_{L^\infty}$ decay over time. There is strong numerical indication that the traveling waves are orbitally asymptotically stable.

Table 2: The decay over time of $\|v(\cdot,t) - v^0(\cdot)\|_{L^1}$ and $\|u(\cdot,t) - u^0(\cdot)\|_{L^\infty}$, where v (and u) represent the numerical solution corresponding to the initial data (48). The norms decay to 0 as $t\to\infty$. Computations using higher resolution and larger times confirmed the result. See also Figure 4.

Time	$\|v - v^0\|_{L^1}$	$\|u - u^0\|_{L^\infty}$
0	1.6527	0.2026
2	0.6540	0.0815
4	0.2005	0.0154
6	0.0399	0.0011
8	0.0061	1.1×10^{-4}

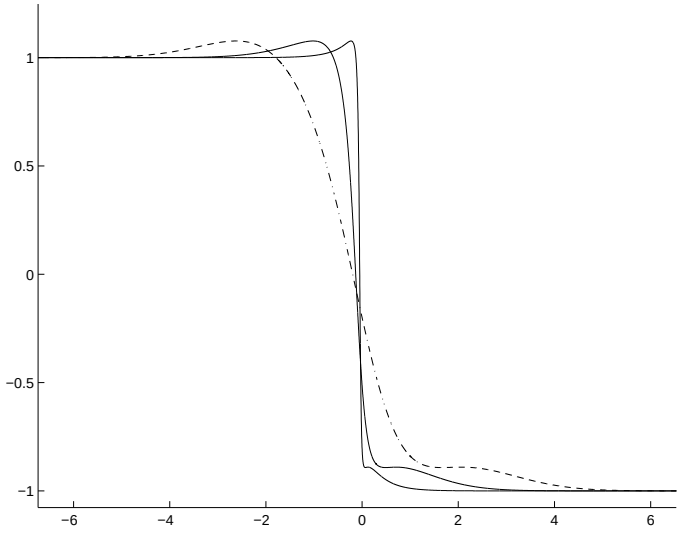

Figure 4: Orbital stability for non-odd initial data. The dash-dot line represents the initial data (48). The profile will approach the unshifted traveling wave v^0 a.e. as $t \to \infty$. The two solid lines represent the solution at $t = 2$ and $t = 4$. The results are confirmed by higher resolution and longer time computations. See also Table 2.

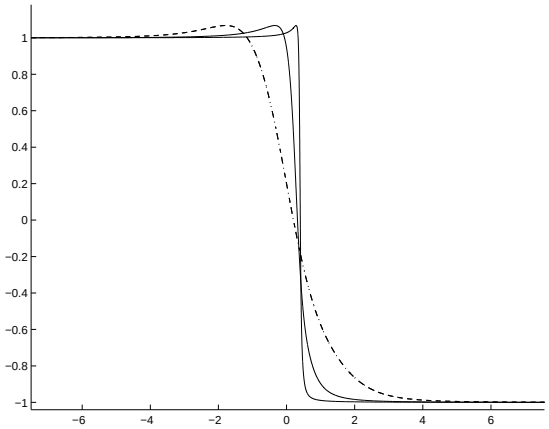

Figure 5: Orbital stability for non-odd initial data. The dash-dot line represents the initial data (49). The profile will approach the shifted traveling wave $\tilde{v}^0(x) = v^0(x + x_0)$, with $x_0 \approx -0.4443$, a.e as $t \to \infty$. The two solid lines represent the solution at $t = 2$ and $t = 4$. See also Table 3.

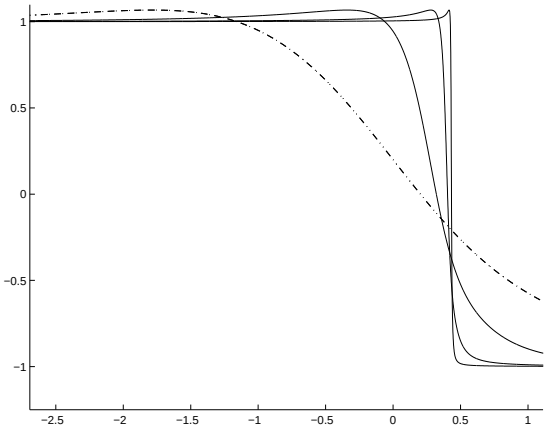

Figure 6: Orbital stability, zoomed around $-x_0 \approx 0.4443$—see Figure 5. The initial data (49) is the dash-dot line. The three solid lines represent the solution at $t = 2$, $t = 4$ and $t = 6$, respectively.

Table 3: The decay over time of the L^1 norm $\|v(\cdot,t) - v^0(\cdot)\|_{L^1}$ and the L^∞ norm $\|u(\cdot,t) - u^0(\cdot)\|_{L^\infty}$. Here, v (and u) represent the numerical solution corresponding to the initial data (49) and $\tilde{v}^0$ and $\tilde{u}^0$ denote the shifted traveling waves $\tilde{v}^0(x) = v^0(x + x_0)$, $\tilde{u}^0(x) = u^0(x + x_0)$ with $x_0 \approx -0.4443$. The norms decay to 0 as $t \to \infty$. Computations using higher resolution and larger times confirmed the result. See also Figures 5 and 6.

Time	$\|v - \tilde{v}^0\|_{L^1}$	$\|u - \tilde{u}^0\|_{L^\infty}$
0	1.6446	0.1948
2	0.5832	0.0606
4	0.1570	0.0145
6	0.0411	0.0044
8	0.0126	0.0018
10	0.0037	7.5×10^{-4}

6 Appendix

The transport equation on the half-line. Consider the first-order transport equation on the negative real axis:

$$f_t + (-d + de^x)\, f_x = 0, \qquad t > 0,\ -\infty < x < 0, \tag{50}$$

with the following initial and boundary conditions:

$$f(x,0) = f_0(x), \quad -\infty < x < 0, \tag{51}$$

$$f(-\infty,t) = 0,\ f(0,t) = d, \quad \text{for all } t > 0. \tag{52}$$

We have an initial-value problem of the type

$$f_t + c(x) f_x = 0, \quad f(x,0) = f_0(x) \tag{53}$$

on the domain $x \in (-\infty, 0)$. For the choice

$$c(x) = -d + de^x,$$

we shall show that the general solution is given by

$$f(x,t) = f_0\left[\log\left(\frac{1}{1 + e^{-dt}[e^{-x} - 1]}\right)\right]. \tag{54}$$

In particular, we note that this solution gives

$$f(0,t) = f_0(0-),$$

and

$$\lim_{x\to-\infty} f(x,t) = \lim_{y\to 0^+} f_0(\log y) = \lim_{x\to-\infty} f_0(x).$$

If $f_0(-\infty) = 0$ and $f_0(0-) = d$, then for all $t > 0$, we would have $f(-\infty,t) = 0$ and $f(0,t) = d$.

Derivation of (54). The solution of (53) may be derived using the method of characteristics. We define $\eta(X,t)$ to be the solution of

$$\partial_t \eta(X,t) = c(\eta(X,t)), \quad \eta(X,0) = X. \tag{55}$$

One may verify that $f(\eta(X,t),t)$ is constant for all t, which implies

$$f(\eta(X,t),t) = f(X,0) = f_0(X). \tag{56}$$

Given $c(x)$, we solve (55) for $\eta(X,t)$. If $\eta(X,\cdot)$ is a diffeomorphism of $(-\infty,0)$, i.e., if there exists a smooth map $\eta^{-1}(x,t)$ such that $\eta(\eta^{-1}(x,t),t) \equiv x$, then by evaluating (56) at $X = \eta^{-1}(x,t)$, we may derive

$$f(x,t) = f_0(\eta^{-1}(x,t)),$$

the solution of the initial-value problem.

Let $c(x) = -d + de^x$. Then, with $g^X(t) = \eta(X,t)$ we may write (55) as

$$\frac{dg}{dt} = d(e^g - 1)$$

Integration gives

$$\int_{g^X(0)}^{g^X(t)} \frac{dg}{e^g - 1} = d \cdot t.$$

(We use $d \cdot t$ to denote the constant d multiplied by the variable t, to avoid confusion with the differential dt.) Let $g = \log y$, note that $g^X(0) = X$, and then compute

$$d \cdot t = \int_{\exp X}^{y^X(t)} \frac{dy}{y(y-1)} = \log \left| \frac{1 - 1/y^X(t)}{1 - 1/\exp X} \right|.$$

Using $y^X(t) = \exp g^X(t) = \exp[\eta(X,t)]$, we have, after some algebra,

$$\eta(X,t) = \log \left(\frac{1}{1 - e^{dt}[1 - e^{-X}]} \right).$$

Now a quick computation shows that

$$\partial_X \eta(X,t) = \frac{e^{dt} e^{-X}}{1 + e^{dt}[e^{-X} - 1]}.$$

Hence we have the following facts:

$$\lim_{X \to -\infty} \eta(X,t) = -\infty$$
$$\eta(0,t) = 0$$
$$\text{For all } X < 0, \quad \partial_X \eta(X,t) > 0$$

This is enough to guarantee that for each t, $\eta(X,t)$ is a diffeomorphism of $(-\infty,0)$. So it is perfectly fine to invert η, which we may do algebraically, resulting in:

$$\eta^{-1}(x,t) = \log \left(\frac{1}{1 + e^{-dt}[e^{-x} - 1]} \right).$$

We then set $f(x,t) = f_0(\eta^{-1}(x,t))$, which is precisely the solution given in(54).

Acknowledgments. We thank Michael I. Weinstein, Tai-Ping Liu, and Joe Keller for discussions and questions regarding this work.

References

[BF] H. S. Bhat and R. C. Fetecau, *A Hamiltonian regularization of the Burgers equation*, J. Nonlinear Sci., to appear.

[CH93] R. Camassa and D. D. Holm, *An integrable shallow water equation with peaked solitons*, Phys. Rev. Lett. **71** (1993), 1661–1664.

[CS00] A. Constantin and W. A. Strauss, *Stability of peakons*, Comm. Pure Appl. Math. **53** (2000), no. 5, 603–610.

[CS02] ———, *Stability of the Camassa-Holm solitons*, J. Nonlinear Sci. **12** (2002), no. 4, 415–422.

[DGH01] H. R. Dullin, G. A. Gottwald, and D. D. Holm, *An integrable shallow water equation with linear and nonlinear dispersion*, Phys. Rev. Lett. **87** (2001), no. 19, 194501.

[DGH03] ———, *Camassa-Holm, Korteweg-de Vries-5 and other asymptotically equivalent equations for shallow water waves*, Fluid. Dynam. Res. **33** (2003), 73–95.

[DGH04] ———, *On asymptotically equivalent shallow water wave equations*, Phys. D **190** (2004), 1–14.

[DHH03] A. Degasperis, D. D. Holm, and A. N. W. Hone, *Integrable and non-integrable equations with peakons*, Nonlinear physics: theory and experiment, II (Gallipoli, 2002), World Sci. Publishing, River Edge, NJ, 2003, pp. 37–43.

[DP99] A. Degasperis and M. Procesi, *Asymptotic integrability*, Symmetry and perturbation theory (Rome, 1998), World Sci. Publishing, River Edge, NJ, 1999, pp. 23–37.

[Goo86] J. Goodman, *Nonlinear asymptotic stability of viscous shock profiles for conservation laws*, Arch. Rational Mech. Anal. **95** (1986), no. 4, 325–344.

[HH05] D. D. Holm and A. N. W. Hone, *A class of equations with peakon and pulson solutions*, J. Nonlinear Math. Phys. **12** (2005), no. suppl. 1, 380–394, With an appendix by H. W. Braden and J. G. Byatt-Smith.

[HS03a] D. D. Holm and M. F. Staley, *Nonlinear balance and exchange of stability in dynamics of solitons, peakons, ramps/cliffs and leftons in a 1+1 nonlinear evolutionary PDE*, Phys. Lett. A **308** (2003), 437–444.

[HS03b] ———, *Wave structure and nonlinear balances in a family of evolutionary PDEs*, SIAM J. Appl. Dyn. Sys. **2** (2003), 323–380.

[HW03] A. N. W. Hone and J. P. Wang, *Prolongation algebras and Hamiltonian operators for peakon equations*, Inverse Problems **19** (2003), 129–145.

[Ise96] Arieh Iserles, *A first course in the numerical analysis of differential equations*, Cambridge University Press, Cambridge, 1996.

[Kur96] P. Kurasov, *Distribution theory for discontinuous test functions and differential operators with generalized coefficients*, J. Math. Anal. Appl. **201** (1996), 297–323.

[Ler34] J. Leray, *Essai sur le mouvement d'un fluide visqueux emplissant l'space*, Acta Math. **63** (1934), 193–248.

[MZM06] K. Mohseni, H. Zhao, and J. E. Marsden, *Shock regularization for the Burgers equation*, 44th AIAA Aerospace Sciences Meeting and Exhibit (Reno, NV), January 2006, AIAA Paper 2006-1516.

[Sat76] D. H. Sattinger, *On the stability of waves of nonlinear parabolic systems*, Advances in Math. **22** (1976), no. 3, 312–355.